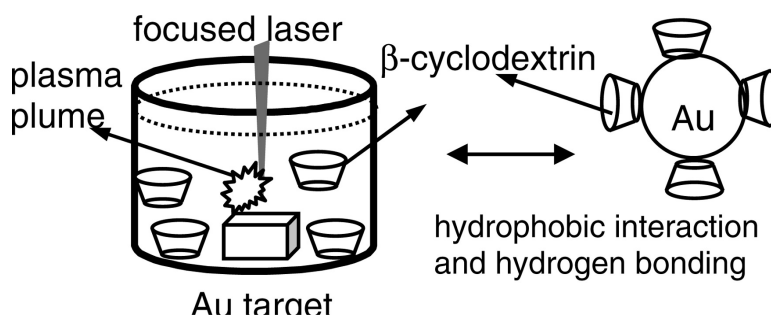Communication

Stabilization and Size Control of Gold Nanoparticles during Laser Ablation in Aqueous Cyclodextrins

Jean-Philippe Sylvestre, Andrei V. Kabashin, Edward Sacher, Michel Meunier, and John H. T. Luong

More About This Article

Additional resources and features associated with this article are available within the HTML version:

- Supporting Information
- Links to the 12 articles that cite this article, as of the time of this article download
- Access to high resolution figures
- Links to articles and content related to this article
- Copyright permission to reproduce figures and/or text from this article

View the Full Text HTML

Stabilization and Size Control of Gold Nanoparticles during Laser Ablation in Aqueous Cyclodextrins

Jean-Philippe Sylvestre,† Andrei V. Kabashin,† Edward Sacher,† Michel Meunier,*,† and
John H. T. Luong*,‡

*Laser Processing Laboratory, Department of Engineering Physics, École Polytechnique de Montréal,
Case Postale 6079, succ. Centre-Ville, Montréal, Québec, Canada, H3C 3A7, and Biotechnology Research Institute,
National Research Council Canada, Montréal, Québec, Canada, H4P 2R2*

Received March 8, 2004; E-mail: michel.meunier@polymtl.ca; john.luong@cnrc-nrc.gc.ca

The laser-induced ablation of a solid target in liquid milieu has become an increasingly popular top-down approach for producing metallic colloids.[1−11] However, the laser ablation of metals in deionized water generally results in rather large (20−300 nm) and highly disperse (50−300 nm) nanoparticles because of the post-ablation coalescence of nanoclusters.[5,12] Surfactants, which interact with the nanoparticles during the condensation and, thus, prevent them from further coalescence and agglomeration, have been used to effectively stabilize and reduce the size of Au and Ag nanoparticles.[5−7] For example, sodium dodecyl sulfate (SDS) was used to produce Au nanoparticles as small as 5 nm.[6] Gold nanoparticles covered with SDS could be problematical for intended biosensing applications, because this surfactant might interfere with the subsequent biomolecule immobilization step.

We recently reported a significant improvement in size reduction and stability of colloidal gold nanoparticles produced by femto-second laser ablation in α-cyclodextrin (CD), β-CD, and γ-CD.[12] This approach offers two key advantages over nanosecond laser ablation: inherent high intensity and low energy to minimize the Joule heating effect. β-CD is most effective in the size control, resulting in monodispersed colloidal particles (2 to 2.5 nm). The colloidal solutions were extremely stable, as reflected by the surface plasmon peak (520 nm), unchanged after 24-month sample storage at room temperature. Such a striking effect of CDs was a pleasant surprise, considering the absence of any obvious chemical interac-tions between CDs and gold colloids. CDs are conical torus-like macrocycles built up from glucopyranose units. Their interior cavity, as well as the primary face, is hydrophobic, while the secondary face and exterior surface are hydrophilic.[13,14] Recently, unmodified CDs were also used to control the size and size distribution of gold nanoparticles prepared by the chemical reduction of HAuCl₄.[15] Uniform particle size was obtained, but the particles were larger than 4−6 nm. In this work, we present new findings to elaborate the nature of CD−nanoparticle interaction.

The ablation of gold was carried out at a fixed fluence in 10 mM β-CD, at pH 3, 5, 6, and 9 (see Supporting Information for detailed information). Only a few seconds into the experiment, the solution prepared at pH > 6 was deep red or pink. At pH < 5, the solution appeared blue-gray, suggesting that much larger particles were produced. The particles prepared at pH > 6 were conspicu-ously stable for several months, while those obtained at pH 3 agglomerated within minutes, as indicated by the color degradation. At high pH values (pH 6 and 9), the mean particle size was about 2.5 nm and the size dispersion did not exceed 1.5 nm fwhm (Supporting Information). In these cases, the mean size and dispersion were almost independent of the pH value (Figure 1). In contrast, particles prepared at low pHs were much larger (20 nm
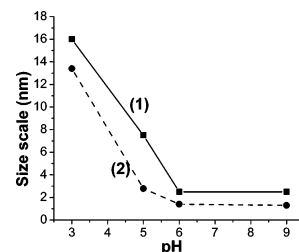
† École Polytechnique de Montréal.
‡ National Research Council Canada.

Figure 1. Mean size (1) and dispersion at fwhm (2) of gold nanoparticles produced in 10 mM β-CD at different pHs.

at pH 3) with broader size dispersions (Supporting Information). Such results could not be explained by the originally proposed mechanism of hydrophobic interactions between gold and the hydrophobic cavity of CD molecules.[12] Notice that the change of pH should not strongly influence the hydrophobic interaction of gold nanoparticles and the hydrophobic cavity of CDs,[13] which possess only −OH groups at pH values below 12.

The surface composition of gold nanoparticles prepared in deionized water was examined by XPS (Supporting Information). A high-resolution spectrum of the gold 4f core level was obtained and can be characterized by three pairs of peaks, each due to spin−orbit coupling (Au⁴f₇/₂ and Au⁴f₅/₂). The analysis of the spectrum reveals partial oxidation of the gold surface. Indeed, while the first and most important pair (BE of 84 and 87.3 eV) is related to elemental gold (Au⁰), the other pairs are related to the only two stable gold oxide states Au⁺ (BE of 85.6 and 89.1 eV) and Au³⁺ (BE of 87.3 and 90.4 eV). On the basis of the relative peak areas of the three different gold compounds, their respective atomic percentages were estimated to be 88.7% for Au⁰, 6.6% for Au⁺, and 4.7% for Au³⁺. With the sensitivity limit of the instrument (1%), the XPS survey scan (0−1000 eV) only reveals the presence of carbon, oxygen, and gold. The presence of carbon is attributed mainly to chemisorbed hydrocarbons (to lower the surface tension of the gold) and to chemisorbed bicarbonates (Au−OCOOH) whose presence was confirmed by FTIR and TOF-SIMS measurements (data not shown). Thus, compounds composed of gold and oxygen are suspected to be present on the surface, leading to a partially hydroxylated surface (Au−OH, pK_a = 3.2) in the presence of water.

The surface charges of the gold nanoparticles were examined by ζ-potential measurements at various pHs in 10 mM NaCl. The measured ζ-potential should be slightly larger than the real surface potential, since it also depends on adsorbed ions of the opposite sign.[16] We observed that the particles produced were negatively charged for all samples. Below pH 5.8, the absolute value of the ζ-potential decreased as the pH decreased, whereas above pH 5.8, the absolute value of the ζ-potential became almost constant (Figure 2). In addition, the experiments at pH below 5.8 were accompanied by a much faster agglomeration of the gold colloids. This process

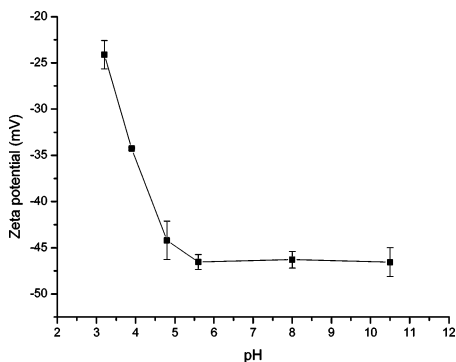**Figure 2.** ζ-Potential measurement as a function of the solution pH.

was especially pronounced at pH 3, where the agglomeration occurred during particle fabrication. Faster agglomeration is consistent with the measured decrease of surface charge, which leads to a reduction of the electrostatic repulsion between negatively charged nanoparticles. The ζ-potential data reveal the presence of a critical point (pH 5.8), very close to the point where the mean particle size drastically changes (Figure 1). Above this point, the mean particle size was much smaller, suggesting that the efficiency of the size reduction is maximal under the relatively high negative charge of the gold surface. Such a charging effect can be explained by the presence of a chemical group able to exchange protons (H^+) with its surrounding environment. In the present case, an equilibrium between $-OH$ and $-O^-$ on the gold surface as the pH is varied is suspected.[17]

The negative charge of the gold surface may be explained by the fact that the Au−OH present on the gold surface can lose protons as the pH increases to form Au−O$^-$ groups on the nanoparticle surface. Hydroxyl groups ($-OH$) are in equilibrium with $-O^-$, and their relative abundance is dictated by the pH value of their environment relative to the pK value of the hydroxylated surface. When the pH is below the pK value, $-OH$ groups are dominant, and when the pH is above, $-O^-$ groups are dominant. Under our experimental conditions, the critical point should be around pH 5 and the oxidized portion of the gold surface should mainly have Au−O$^-$ groups at pH > 5 and increasing numbers of Au−OH groups at pH < 5. A similar model has already been used to explain the ζ-potential measurements of gold thin films[17] and gold nanoparticles produced by ultrasonic agitation, in aqueous media, of a vacuum-evaporated gold thin film.[18] The presence of $-OH$ or $-O^-$ on the gold particles makes hydrogen bonding with CDs possible. CDs possess only $-OH$ groups on both conical faces (at pH values <12). It means that effective hydrogen bonding between gold and CDs is possible only when $-O^-$ groups are present on the gold surface (in contrast, the bonding is not effective when $-OH$ groups are dominant on the gold surface because of the much weaker interaction between two $-OH$ groups). This mechanism can explain the pH dependence of the nanoparticle size. Indeed, the formation of O$^-$ takes place only at relatively high pH > 5, which corresponds to the reduction of gold nanoparticle size in our experiments. In addition to stronger hydrogen bonding at pH > 5, the high absolute value of the surface charge of the particles fabricated in such experimental conditions could also be implicated in the production of smaller particles. Highly negatively charged nanoparticles can repel each other more effectively, thus allowing the CD molecules to cover them before contact occurs. These kinetics considerations are expected to limit the coalescence of the forming clusters, leading to smaller particles. The presence of hydrogen bonding was also confirmed by the comparison of the FTIR spectra of pure β-CD and that of gold nanoparticles fabricated

in 10 mM β-CD (pH 6) (Supporting Information). The $-OH$ stretching mode absorption band shifts 27 cm^{-1} lower for gold particles in the presence of β-CD. Such a shift is generally attributed to the increase in the strength of intermolecular hydrogen bonding.[19]

Thus, a model considering the partially hydroxylated nature of the gold surface and possible hydrogen bonding with CDs unambiguously explains pH dependencies for the nanoparticle size and size dispersion. However, this model cannot explain why β-CD is much more efficient in nanoparticle size reduction and in solution stabilization than either γ-CD or α-CD. As discussed earlier, the gold surface is only partially oxidized or hydroxylated. The rest of the gold surface should be metallic, i.e., essentially hydrophobic. CDs are also known to be hydrophobic in the cavity interior and on the primary face. In fact, the hydrophobicity is related to the solubility of substances in aqueous solutions. Considering the solubility of different types of CDs with 0.016, 0.149, and 0.179 mol/L for β-CD, α-CD, and γ-CD, respectively, we may conclude that β-CD has a much higher hydrophobicity than either α-CD or γ-CD. As a result, β-CD is capable of forming much stronger hydrophobic complexes with metallic gold to minimize the total energy of the system, in agreement with our experimental results.[12] The results for the other types of CDs are probably explained by the interplay of the two proposed mechanisms with a much greater ability for hydrophobic interactions for β-CD (β-CD > γ-CD > α-CD) and a greater ability for hydrogen-bonding reactions for CDs with a larger number of $-OH$ groups on their primary surfaces (8, 7, and 6 groups for γ-CD, β-CD, and α-CD, respectively). The CD molecules cover gold nanoclusters just after ablation and act as "bumpers", limiting contact between particles, preventing their coalescence (when the particles are still "hot") and aggregation (when the particles are "cold").

Supporting Information Available: Detailed information on laser ablation, instrumentation techniques, TEM imaging, and the FT-IR and XPS spectra of gold nanoparticles. This material is available free of charge via the Internet at http://pubs.acs.org.

References

(1) Fojtik, A.; A. Henglein, A. *Ber. Bunsen-Ges. Phys. Chem.* **1993**, *97*, 252.
(2) Henglein, A. *J. Phys. Chem.* **1993**, *97*, 5457.
(3) Sibbald, M. S.; Chumanov, G.; Cotton, T. M. *J. Phys. Chem.* **1996**, *100*, 4672.
(4) Compagnini, G.; Scalisi, A. A.; Puglisi, O. *Phys. Chem. Chem. Phys.* **2002**, *4*, 2787.
(5) Mafune, F.; Kohno, J.-Y.; Takeda, Y.; Kondow, T.; Sawabe, H. *J. Phys. Chem. B* **2000**, *104*, 9111.
(6) Mafune, F.; Kohno, J.-Y.; Takeda, Y.; Kondow, T.; Sawabe, H. *J. Phys. Chem. B* **2001**, *105*, 5114.
(7) Chen, Y.-H.; Yeh, C.-S. *Colloids Surf., A* **2002**, *197*, 133.
(8) Dolgaev, S. I.; Simakin, A. V.; Voronov, V. V.; Shafeev, G. A.; Bozon-Verduraz, F. *Appl. Surf. Sci.* **2002**, *186*, 546.
(9) Tsuji, T.; Iryo, K.; Watanabe, N.; Tsuji, M. *Appl. Surf. Sci.* **2002**, *202*, 80.
(10) Tsuji, T.; Kakita, T.; Tsuji, M. *Appl. Surf. Sci.* **2003**, *206*, 314.
(11) Kabashin, A. V.; Meunier, M. *J. Appl. Phys.* **2003**, *94*, 7941.
(12) Kabashin, A. V.; Meunier, M.; Kingston, C.; Luong, J. H. T. *J. Phys. Chem. B* **2003**, *107*, 4527.
(13) Szejtli, J. In *Comprehensive Supramolecular Chemistry*; Atwood, J. L., Davies, J. E. D., Macnicol, D. D., Vogtle, F., Eds.; Pergamon-Elsevier: New York, 1996; Vol. 3.
(14) Szejtli, J. *Chem. Rev.* **1998**, *98*, 1743.
(15) Liu, Y.; Male, K. B.; Bouvrette, P.; Luong, J. H. T. *Chem. Mater.* **2003**, *15*, 4172.
(16) Evans, D. F.; Wennerström, H. *The Colloidal Domain Where Physics, Chemistry, Biology, and Technology Meet*, 2nd ed.; Wiley-VCH: New York, 1999; p 632.
(17) Duval, J.; Huijs, G. K.; Throels, W. F.; Lyklema, J.; van Leeuwen, H. P. *J. Colloid Interface Sci.* **2003**, *260*, 95.
(18) Thompson, D. W.; Collins, I. R. *J. Colloid Interface Sci.* **1992**, *152*, 197.
(19) Bellamy, L. J. *The Infrared Spectra of Complex Molecules*; Chapman and Hall: London, 1975.

JA048678S